Research Square

Preprints are preliminary reports that have not undergone peer review.
They should not be considered conclusive, used to inform clinical practice,
or referenced by the media as validated information.

Spatial Co-benefits of Forest Biomass Density and Structural Diversity in Indonesia with GEDI

Paromita Basak

pbasak@umd.edu

University of Maryland College Park (UMD) https://orcid.org/0009-0005-3240-5787

Tiago de Conto

University of Maryland College Park (UMD)

Wenlu Qi

University of Maryland College Park (UMD)

Ralph Dubayah

University of Maryland College Park (UMD)

Patrick Roehrdanz

Conservation International https://orcid.org/0000-0003-4047-5011

Matthew Hansen

Wahyu Adinugroho

Haruni Krisnawati

Sigit Sasmito

Laura Duncanson

Article

Keywords:

Posted Date: June 18th, 2026

DOI: https://doi.org/10.21203/rs.3.rs-9951857/v1

License: This work is licensed under a Creative Commons Attribution 4.0 International License.
Read Full License

Additional Declarations: There is **NO** Competing Interest.

Paper Title: Spatial Co-benefits of Forest Biomass Density and Structural Diversity in Indonesia with GEDI

Authors: Paromita Basak[1]*, Tiago de Conto[1], Wenlu Qi[1], Ralph Dubayah[1], Patrick R. Roehrdanz[2], Matthew C. Hansen[1], Wahyu Catur Adinugroho[3], Haruni Krisnawati[4], Sigit D. Sasmito[5], Laura Duncanson[1]

Affiliations

[1] Department of Geographical Sciences, Center for Geospatial Information Science, University of Maryland, College Park, MD, USA

[2] Moore Center for Science and Solutions, Conservation International, Arlington, VA 22202, USA

[3] Research Center for Ecology, National Research and Innovation Agency (BRIN), Jl. Raya Jakarta–Bogor, Cibinong 16911, Bogor, West Java, Indonesia

[4] Ministry of Forestry, Jakarta, Indonesia

[5] Centre for Tropical Water and Aquatic Ecosystem Research (TropWATER), Townsville, QLD, Australia

Corresponding author: Paromita Basak, pbasak@umd.edu

Abstract:

Natural climate solutions, including ecosystem conservation and restoration, are central to achieving global climate mitigation goals while supporting biodiversity and ecosystem resilience. Areas of high carbon and biodiversity offer opportunities to maximize conservation impact. We identify structural co-benefit areas across Indonesia's ecoregions using satellite lidar and assess their protection status and exposure to risk. Approximately 90,000 km² of co-benefit areas were identified, containing 4.3 ±0.001 Pg of aboveground biomass. Only 22% of these areas are formally protected, with ~78% remain unprotected; one third of unprotected co-benefit areas are within 10 km of major roads, indicating elevated risk of future loss. Rainforest and swamp forest hotspots remain particularly underprotected. We estimate that 1.4 ±0.001 Pg of biomass occurs in elevated risk unprotected co-benefit areas. These findings highlight conservation opportunities in Indonesia's most carbon-dense, diverse ecosystems and support targeted conservation planning to advance Indonesia's Nationally Determined Contribution and the global 30×30 target.

1. Introduction

The ongoing climate and biodiversity crises pose significant threats to ecosystems and human society [1,2]. Forested ecosystems contain 80–90% of global plant biomass as well as a significant portion of Earth's terrestrial biodiversity, encompassing the majority of terrestrial plant and animal species [3] and are therefore crucial for mitigating and adapting to climate change [4,5]. It is particularly important to understand and monitor the dynamics of aboveground biomass density (AGBD) in tropical forests, which store large magnitudes of carbon (more than 200 Pg C) [6] and host at least two-thirds of the world's flora and fauna diversity [7]. Due to their substantial capacity for carbon sequestration and storage, forest conservation and restoration in these tropical rainforests serve as effective nature-based strategies for mitigating atmospheric carbon levels [8]. Protection and restoration of tropical rainforest systems has the potential to sequester approximately 226 Gt C from the atmosphere [4], which would effectively offset the estimated median remaining carbon budget of ~120 Gt C emissions from 2020 onward in order to limit global temperature increases to 1.5 degrees [9]. Achieving these climate and biodiversity objectives, however, requires robust, spatially explicit approaches for monitoring forest carbon stocks and ecosystem conditions across tropical landscapes.

The arrival of NASA's GEDI (Global Ecosystem Dynamics Investigation) LiDAR (Light Detection and Ranging) mission [10] provides a step change in Earth Observation (EO) capabilities for forest biomass and structural diversity mapping –particularly when employing a fusion of GEDI and Synthetic Aperture Radar (SAR) data such as from DRL's TanDEM-X missions [11], which are valuable for Indonesian forest structure mapping because of its sensitivity to canopy volume and its ability to penetrate cloud cover, a critical limitation in tropical regions [12]. GEDI-SAR fusion has also enabled mapping of structural diversity which is commonly defined as the variability of the three-dimensional spatial arrangement of trees and other structural elements within a forest [13,14]. Beyond improving forest monitoring, these advances provide an unprecedented opportunity to examine the ecological significance of forest structure at regional to global scales.

The widely cited habitat heterogeneity hypothesis suggests that structurally diverse forests support greater species diversity by providing more niches and habitats [15–17]; for instance, indices

of structural heterogeneity correlate with richness of birds and vascular plants [18], old-growth stand features such as cavity-bearing trees enhance vertebrate functional diversity [19], and abundant deadwood and vertical complexity are linked to higher invertebrate diversity [20]. In old-growth forests, persistent structural heterogeneity (e.g., canopy layering, large trees, dead wood, and gap dynamics) [14,21] creates stable habitat niches that are occupied by different species across multiple taxonomic groups, leading to higher biodiversity over time [19,22]. More recently, spaceborne lidar has enabled the relationship between them to be tested at much larger scales, and GEDI-derived canopy metrics have been shown to predict multiple dimensions of avian diversity across North America, including species richness and functional diversity [23] . While these findings demonstrate the potential of structural diversity as a biodiversity-relevant metric, most studies remain geographically restricted, focused on a single taxonomic group, and have yet to evaluate whether structural indices, such as GEDI waveform metrics or ALS-derived products can function as general biodiversity proxies in tropical forests. Importantly, the habitat heterogeneity hypothesis does not always hold true [24] as some studies have shown structural diversity is not always positively related to forest biomass and maturity. Disturbances such as non-stand-replacing fires can induce mixed-aged structures [25], thus increasing structural diversity in disturbed forests which does not necessarily indicate higher species diversity. Therefore, while structural diversity offers considerable promise as a scalable proxy for biodiversity, further research is needed to better understand the relationships among biodiversity, habitat quality, and forest structural diversity, particularly in tropical forest ecosystems. Identifying where high carbon stocks and biodiversity-relevant structural complexity coincide is particularly important for informing conservation strategies aimed at maximizing multiple ecosystem benefits.

While the Conference of Parties to the Convention on Biological Diversity (CBD) in Montreal, Canada, resulted in nations' commitment in protecting 30% of their lands and seas by 2030 (the '30 × 30 goal') [26], the effectiveness of global protected areas (PAs) regarding conserving vulnerable biodiversity and habitats remains uncertain [27,28]. Although the primary goal of most established global PAs has been biodiversity conservation [29], there are significant co-benefits for carbon storage, as older, biodiverse forests tend to sequester more carbon [30–32]. Here, co-benefits are defined as areas where the conservation of biodiversity (e.g., species-rich or structurally diverse forests) aligns with high carbon storage, enabling PAs to deliver multiple environmental benefits [30,31]. These PA benefits often include preventing forest cover loss across various regions [33–35],

regulating local climate and temperature [36], and potentially enhancing carbon sequestration capacity [37,38]. Expanding PAs could therefore serve as a strategy for strengthening climate change mitigation efforts [39]. Protected forests are estimated to account for approximately 27% of the net global greenhouse gas sink [40], noting that 'protected' does not necessarily imply 'intact,' as many PAs include secondary or partially degraded forests. Nevertheless, substantial uncertainties remain regarding stocks and fluxes in terrestrial ecosystems [41,42]. Recent research estimated the total aboveground carbon (C) stock within PAs at 61.43 Gt (±0.31), accounting for 26% of all mapped terrestrial woody carbon [43]. Of this, an additional 9.65 ± 0.88 Gt C was attributed to PA status, primarily due to avoided emissions from deforestation and degradation compared to unprotected forests [43]. To meet the '30 × 30 goal', more research needs to be done for each country's PA efficiency and determine how much carbon and biodiversity can be protected further to reduce emissions. In this context, it is essential to consider global PA frameworks into national governance systems, as definitions and management objectives may be different across countries. Indonesia provides a relevant case study, where the forest estate (Kawasan Hutan) is divided into production, protection, and conservation forests under Law No. 41/1999 [44]. This country provides an especially compelling research scope for evaluating how effectively PAs safeguard both carbon and biodiversity co-benefits.

Around 15% of the Earth's tropical forests are situated in South-East Asia (SEA) and contain at least 4 out of the 25 biodiversity hotspots that are globally indispensable [45,46]. Hence, for supporting global conservation goals, it is critical to assess the performance and spatial coverage of PAs across SEA to inform evidence-based conservation planning. Recent studies on PAs in Indonesia have shown to reduce deforestation rates compared to surrounding areas, although they may still experience pressures and are not fully immune to forest loss [47]. A remote sensing-based PA study in Indonesia, which used data from 2000-2010, has shown that PAs with exclusive focus on biodiversity have shown variable effectiveness in slowing deforestation rates, depending on management capacity, location, and external pressures [48]. In Kalimantan, protected lowland forests declined by 56% from 1985 to 2001[49], with over 2 Mha of forest lost in proposed and existing PAs between 1996 and 2002 [50]. The PAs in this region are becoming more isolated while the surrounding landscapes experience increasing degradation and deforestation [49]. On the other hand, rates of deforestation with Sumatran PAs between 1990-2000 were seen to be lower than adjacent unprotected areas [48]. Moreover, high leakage is reported around PAs such as Bukit Tigapuluh

National Park, where only 10.21% of the forest in the buffer zone remained due to its proximity to the PA [51]. More recent regional assessments indicate that PAs in SEA generally experience lower forest loss than comparable unprotected lands, but their effectiveness remains highly variable across locations and anthropogenic pressures [27,28]. Additionally, most contemporary studies continue to focus primarily on forest cover change, with limited assessment of whether PAs simultaneously protect forest carbon stocks and biodiversity-relevant structural complexity at regional scales, particularly using emerging remote sensing technologies, such as, spaceborne lidar observations. Addressing this gap requires spatially explicit assessment of whether existing PA networks effectively capture areas where forest carbon and biodiversity-relevant structural complexity converge.

Here, we investigate the spatial coincidence between high forest carbon stock areas and high structural diversity across Indonesian ecoregions, identifying zones of carbon-biodiversity 'co-benefits'. Specifically, we quantify the proportion of these co-benefit areas that fall within existing PAs versus those that remain unprotected, and examine how this varies across ecoregions. In doing so, we address a critical knowledge gap regarding the spatial coincidence between forest biomass and structural diversity, and evaluate the potential for simultaneously advancing aboveground carbon storage and biodiversity conservation goals in one of the world's most biodiverse and carbon-rich tropical nations.

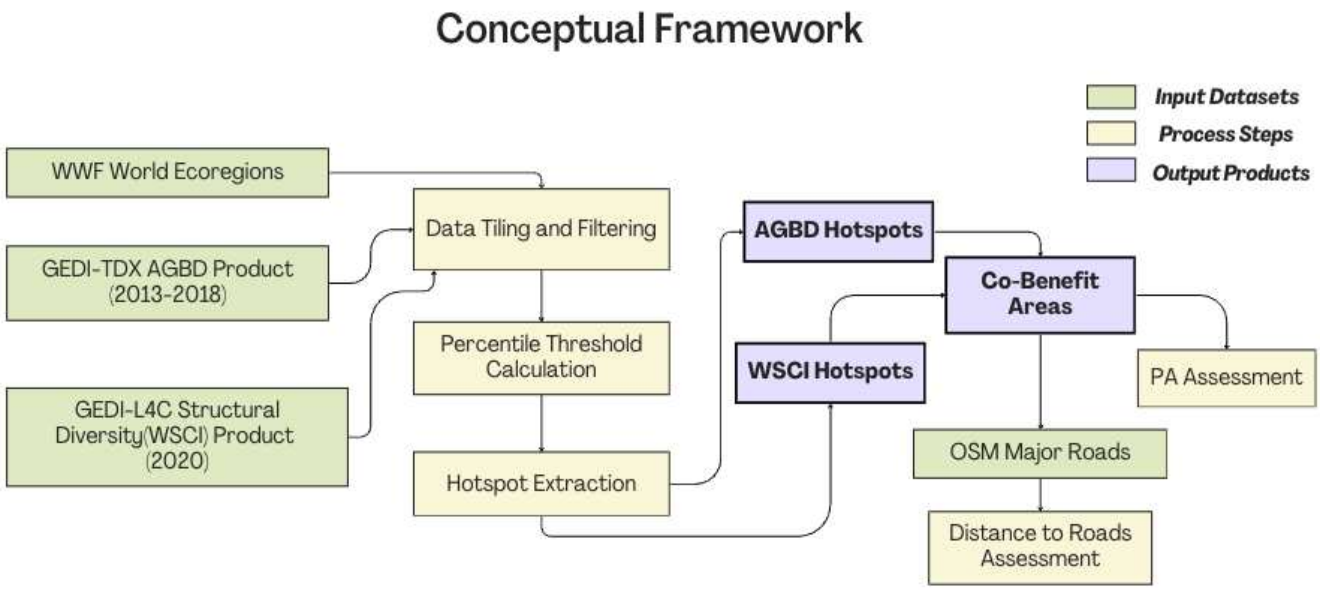


***Figure 1:** A conceptual framework for identifying and assessing forest biomass carbon and structural diversity co-benefit hotspots in tropical forests. The workflow begins by processing three core datasets: World Wildlife Fund (WWF) World Ecoregions to define the target ecosystem, and two wall-to-wall GEDI-derived layers—Aboveground Biomass Density (AGBD, GEDI-TDX) and Waveform Structural Complexity Index (WSCI, GEDI-SAR). Following data tiling and filtering, we apply a percentile-based threshold approach (top 10%) for each product to define 'Hotspot Extraction.' The spatial intersection of these two hotspot layers identifies our key priority output: "Co-Benefit Areas". Finally, we first analyze co-benefits withinWorld Database of Protected Areas(WDPA), and as a distance to OpenStreetMap (OSM) Major Roads.*

2. Results

We mapped co-benefit hotspots across 38 terrestrial ecoregions derived from WWF using wall-to-wall remote sensing products (Table 1). Ecoregion specific and national percentile thresholds were used to delineate areas of high (top 10%) aboveground carbon storage and structural complexity, and their spatial overlap was used to identify carbon-structural diversity co-benefit areas. We then assessed the extent to which these priority areas are currently represented within the protected area network of Indonesia and evaluated their exposure to potential anthropogenic pressures (Figure 1).

2.1 Co-benefit areas Selection and Significance

The total co-benefit area in Indonesia is ~90,000 km² (Figure 2). We found different spatial patterns in the AGBD and structural diversity maps, with 34.7% of the higher spatial resolution WSCI (structural diversity) hotspots overlap with AGBD hotspots, and 62.7% of AGBD hotspots

overlap with WSCI hotspots. This reflects stronger spatial clustering of structural diversity hotspots relative to the broader distribution of AGBD hotspots, indicating that many high-biomass forests occur outside the most structurally complex regions, whereas structurally diverse forests tend to form more spatially concentrated hotspot clusters.

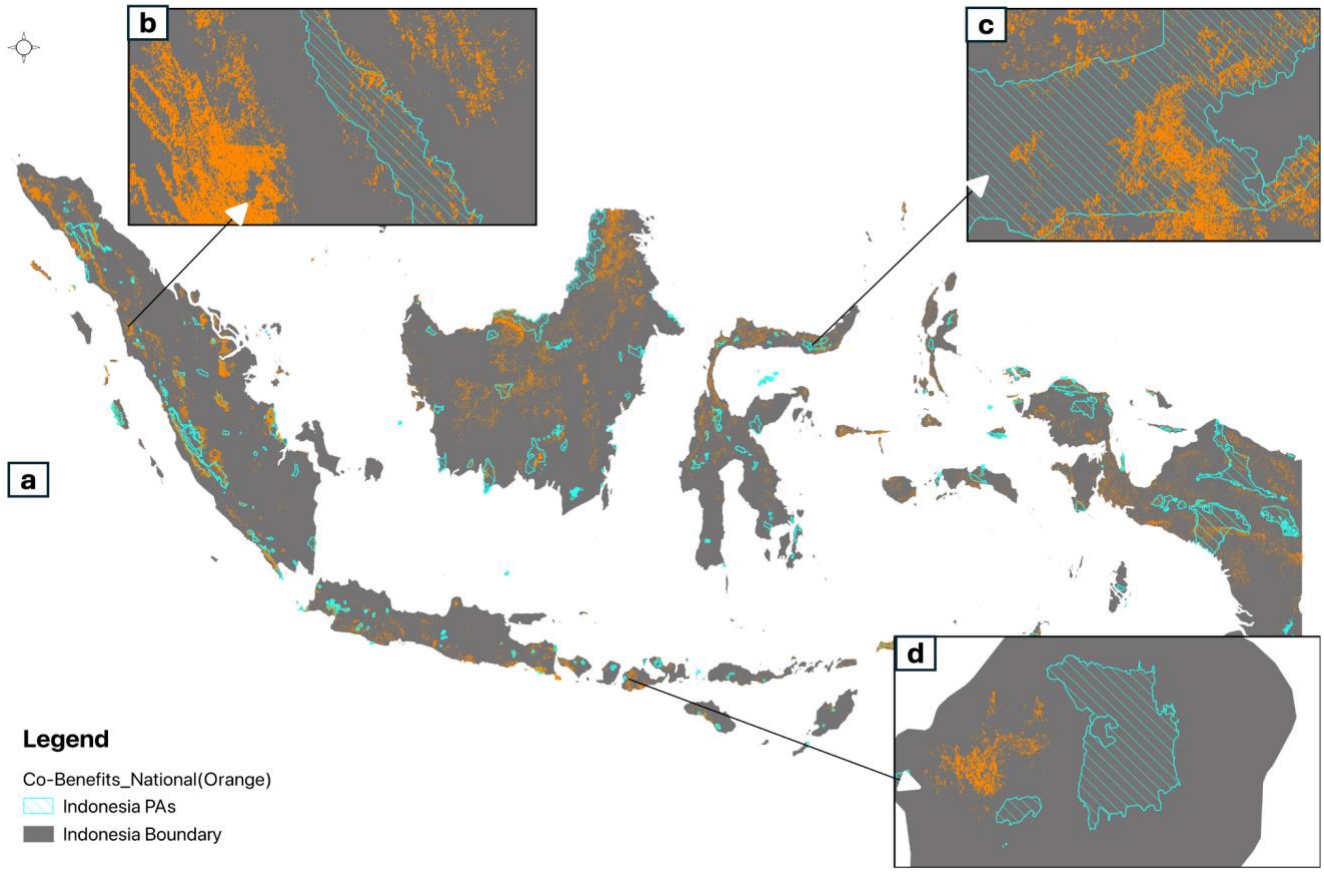


Figure 2: Spatial distribution of ecoregion-threshold based co-benefit areas across Indonesia.

The map shows detected co-benefit areas (panel a), defined as regions exhibiting both high aboveground biomass density (AGBD) and high structural diversity. Inset maps illustrate protected areas with varying levels of co-benefit overlap: Barumun Wildlife Reserve (panel b; Sumatran Montane and Lowland Rain Forests), Bogani Nani Wartabone National Park (panel c; Sulawesi Montane and Lowland Rain Forests), and Gunung Rinjani National Park, Kerandangan Nature Recreation Park, and Nuraksa Grand Forest Park (panel d; Lesser Sundas Deciduous Forests).

Bukit Raya National Park in Borneo, Indonesia, presents an illustrative example of our results (Figure 3). which is also a part of the Schwaner mountain range at the border of Central and West Kalimantan. This park is a part of the Schwaner mountain range at the border of Central and West Kalimantan, and included in the 'Heart of Borneo Project' by WWF for Nature. The park

contains both AGBD hotspots (Figure 3a) and WSCI hotspots (Figure 3b) within the park boundary, with their intersection resulting in 100m resolution cell clusters of co-benefit areas (Figure 3c). The maps show that a significant proportion of high AGBD and WSCI hotspots along with the co-benefit areas are within the protected area, but expansion would cover neighboring co-benefit areas.

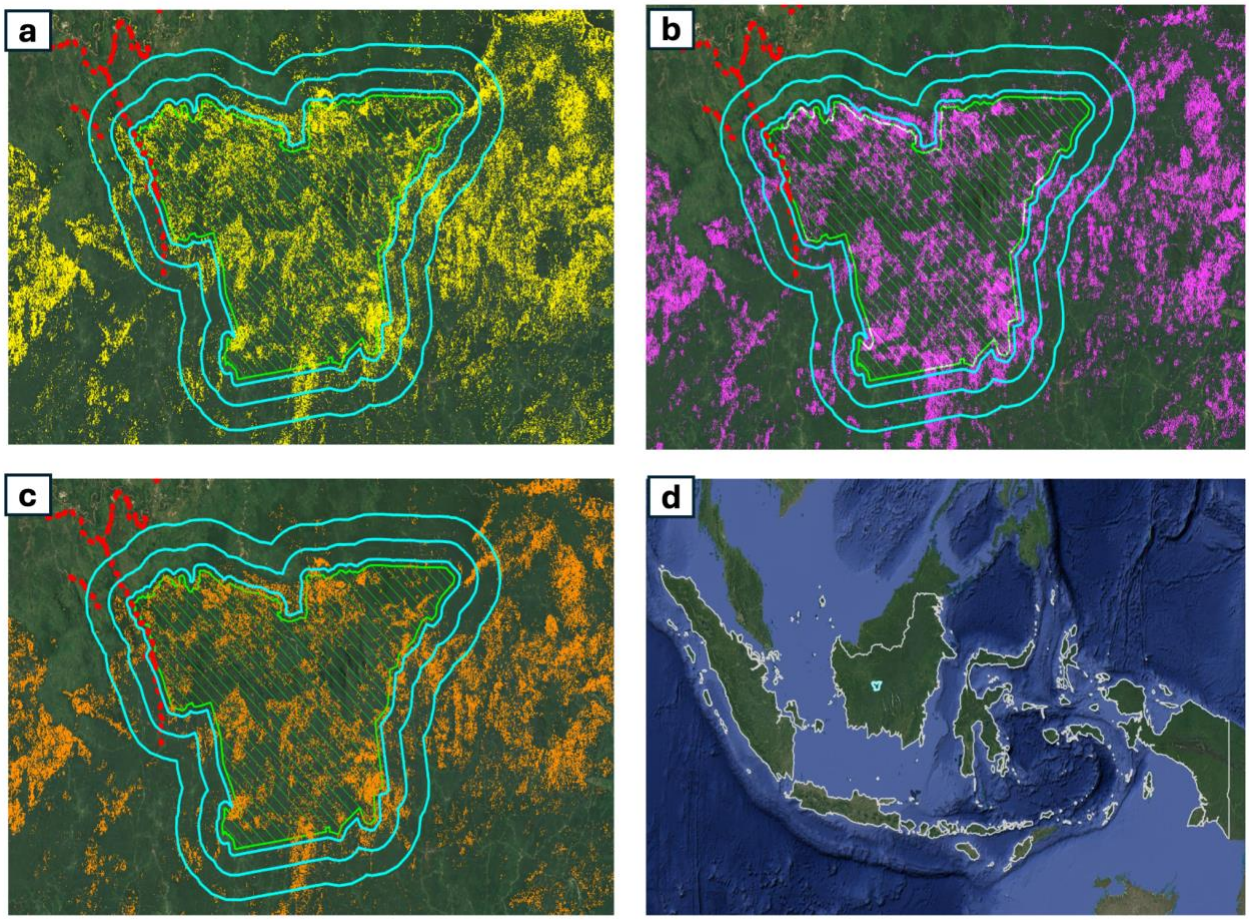


Figure 3: Spatial distribution of AGBD hotspots, WSCI hotspots, and co-benefit areas in Bukit Raya National Park, Indonesia.
(a) AGBD/Biomass hotspots (yellow) with (1, 5, and 10 km; cyan) and major roads (red).
(b) WSCI/Structural Diversity hotspots (fuchsia) with buffer zones and major roads (red).
(c) Co-benefit areas (orange), representing overlap between AGBD and WSCI hotspots, with buffer zones and major roads (red).
(d) Location of the park(cyan) within the national boundary (gray).
Bukit Raya National Park is located in the Schwaner Mountain range at the border of Central and West Kalimantan and forms part of the "Heart of Borneo" conservation initiative.

The PA assessment of the co-benefit areas (Figure 4a) shows that only ~22% of co-benefit areas are inside PAs where a large majority (~78%) of them remain outside WDPA-defined PAs,

although some of these areas may still be managed under other forest management or conservation-related frameworks that were not explored in this research.

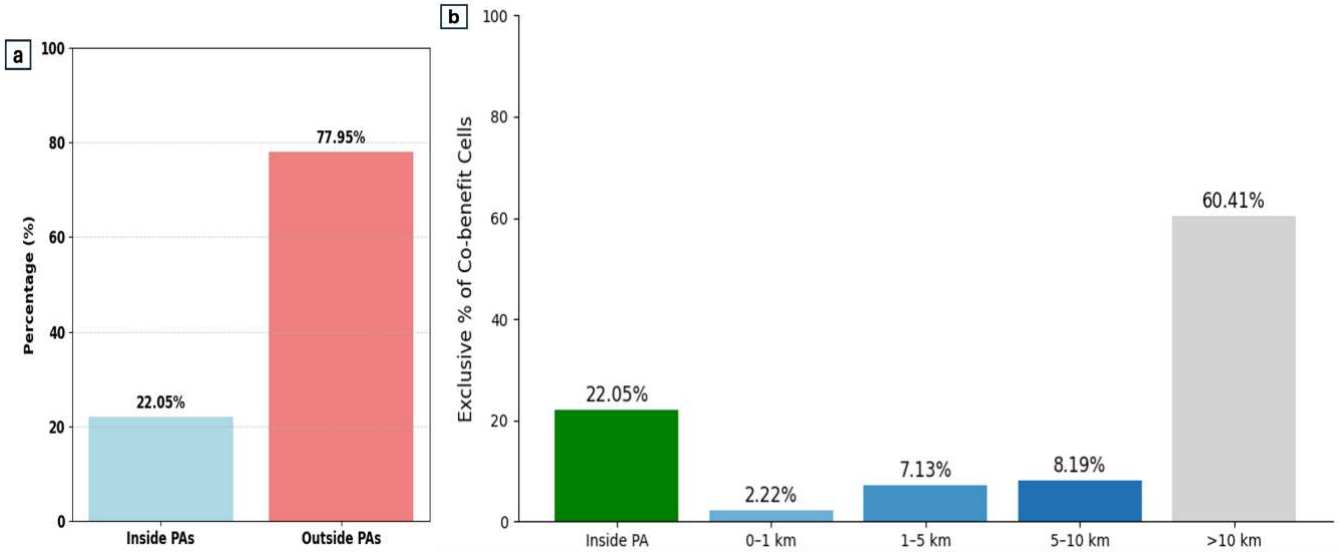


Figure 4: Spatial distribution of co-benefit areas relative to protected areas (PAs).

(a) Proportion of total co-benefit area located inside and outside existing protected areas, showing that a majority of high-carbon and structurally diverse forests occur outside the current PA network.
(b) Distribution of co-benefit areas by distance from PA boundaries, indicating the proportion of areas located within 0–1 km, 1–5 km, 5–10 km, and >10 km of protected areas.
Together, these results highlight the spatial separation between co-benefit forests and existing protection, with a large fraction of high-priority areas occurring beyond immediate PA influence.

The PA buffer zone analysis of the co-benefit areas indicates 22% being located inside PAs, while only 2.2% are found within 1 km of PA boundaries (Figure 4b). An additional 7.1% and 8.2% are located within 1–5 km and 5–10 km of PAs, respectively. The majority, however, lie beyond 10 km from any PA, accounting for 60.4% of all co-benefit areas.

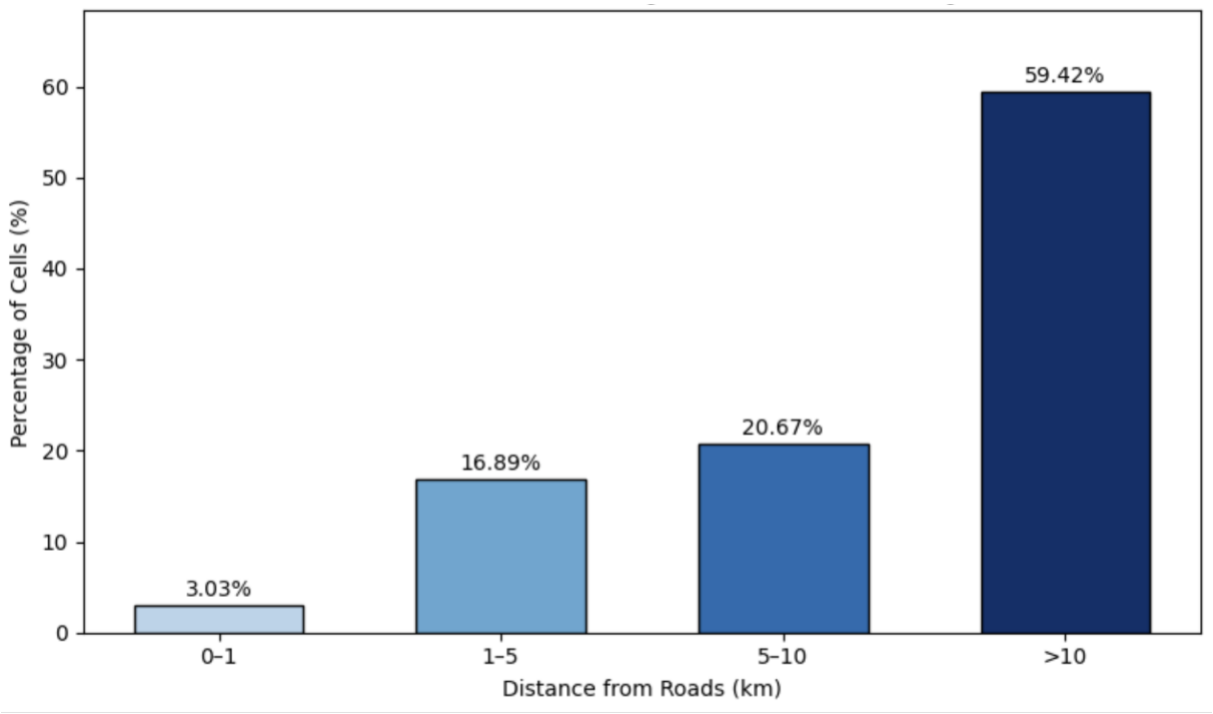


Figure 5: Percentage of co-benefit areas relative to distance from major roads.

More than half of the total co-benefit areas are located more than 10 km from existing OSM derived road networks.

In this research, we also conducted a preliminary risk assessment of the co-benefit areas relative to the nearby major roads derived from OpenStreetMap (OSM). The distribution of co-benefit areas by their distance from major roads shows that ~3% are located within 1 km, ~17% between 1–5 km, and ~21% between 5–10 km (Figure 5). The majority of co-benefit areas (~59%) are situated more than 10 km away from roads (Figure 5). Further assessment reveals that while ~40% of co-benefit areas are within 10 km of a road, 11% of those are within 10km of a PA which can result in key conservation opportunities to expand existing networks to target these proximal co-benefit areas.

Table 2: AGB distribution within Co-Benefit areas and AGBD/biomass hotspots by protected area status.

Hotspot Category	*Total hotspot area (km²)*	*Total AGB (Pg)*	*AGB inside PAs (Pg)*	*AGB outside PAs (Pg)*
Co-benefit areas	~90,000	4.3 ± 0.001	0.9 ± 0.001	3.4 ± 0.001
Biomass (AGBD) hotspots	~176,000	6.9 ± 0.001	1.4 ± 0.001	5.6 ± 0.001

Our assessment shows that the co-benefit areas contain approximately 4.3 ±0.001 Pg of AGB, of which ~79% occurred outside existing protected areas (Table 2).

Below, we separately consider results in AGBD and structural diversity hotspots as some conservation priorities focus on carbon or biodiversity initiatives independently.

2.2 AGBD (Carbon) Hotspots

We identified a total of ~143,200 km² of forest AGBD hotspots for all ecoregions in Indonesia (Figure 6). These hotspots represent areas where AGBD is among the top 10% within each ecoregion and are spatially mapped across the country alongside the WDPA protected area layer (Figure 6).

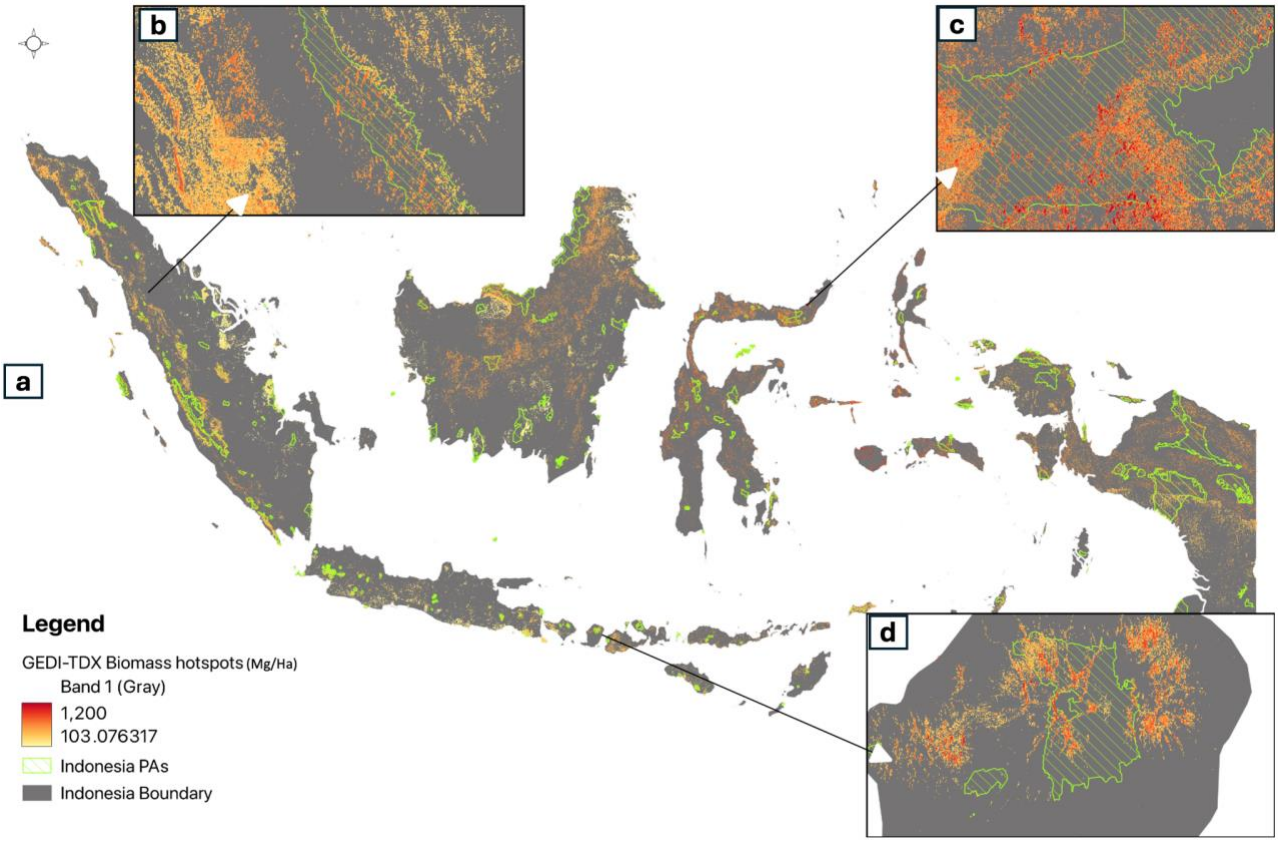


Figure 6: Spatial distribution of aboveground biomass density (AGBD) hotspots across Indonesia.

The map shows AGBD (Mg/ha) hotspots (100m) for each ecoregion (panel a). Inset maps show example protected areas : Barumun Wildlife Reserve (panel b; ecoregion: Sumatran Montane and Lowland Rain Forests), Bogani Nani Wartabone National Park (panel c; ecoregion: Sulawesi Montane and Lowland Rain Forests), and Gunung Rinjani National Park, Kerandangan Nature Recreation Park, and Nuraksa Grand Forest Park (panel d; ecoregion: Lesser Sundas Deciduous Forest).

2.3 Structural Complexity Hotspots:

The Structural Diversity layer (WSCI) identifies ~168,000 km² of hotspot areas, representing regions where WSCI values fall within the top 10% of each ecoregion (Figure 7). These hotspots correspond to WSCI values ranging between 10.44 and 11.39 (see Supplementary Figure S2), aligning with the highest structural diversity ranges reported for tropical forest biomes [52]. Spatially, WSCI hotspots exhibit more pronounced clustering across Indonesia compared to AGBD hotspots.

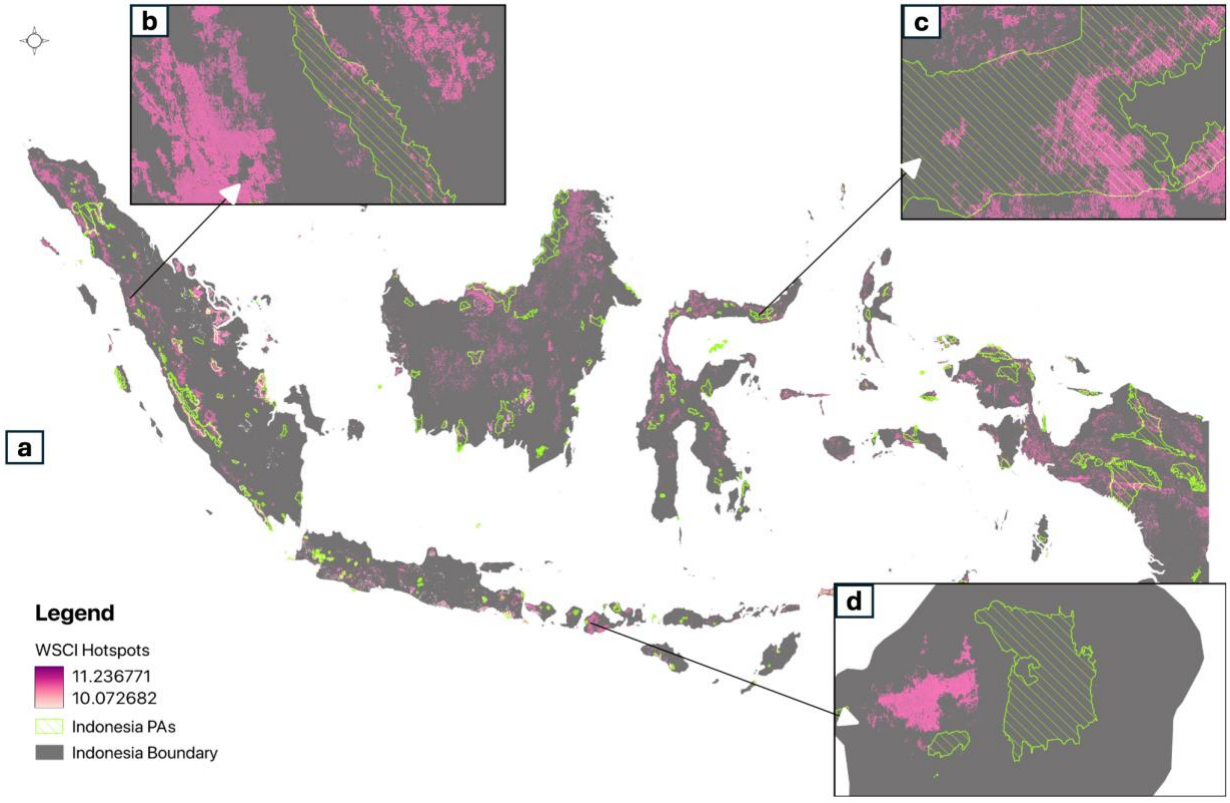


Figure 7: Spatial distribution of structural diversity (WSCI) hotspots across Indonesia.

The map shows GEDI-L4C based hotspots (Fuchsia) where the selected hotspots(25m) threshold(panel a). Inset maps show the same protected area examples as Figure 6.

2.4 PA vs Non-PA Assessment of AGBD hotspots

The GEDI-TDX hotspot assessment identified ~176,000 km² of high-biomass forest containing approximately 6.9 ±0.001 Pg of AGB, with nearly 80% occurring outside existing PAs (Table 2; Figure 8a).

For further assessment of ecoregion-specific differences in AGB between PAs and non-PAs, ecoregions were divided based on their primary vegetation types. These categories include

rainforests, swamp forests, deciduous forests, heath forests, mangroves, grasslands and pine forests. Again, the analysis shows that a significant proportion of biomass hotspots are located outside of PAs (Figure 8b). Many high-AGB areas, such as rainforests, which are crucial for carbon storage and biodiversity conservation, remain unprotected.

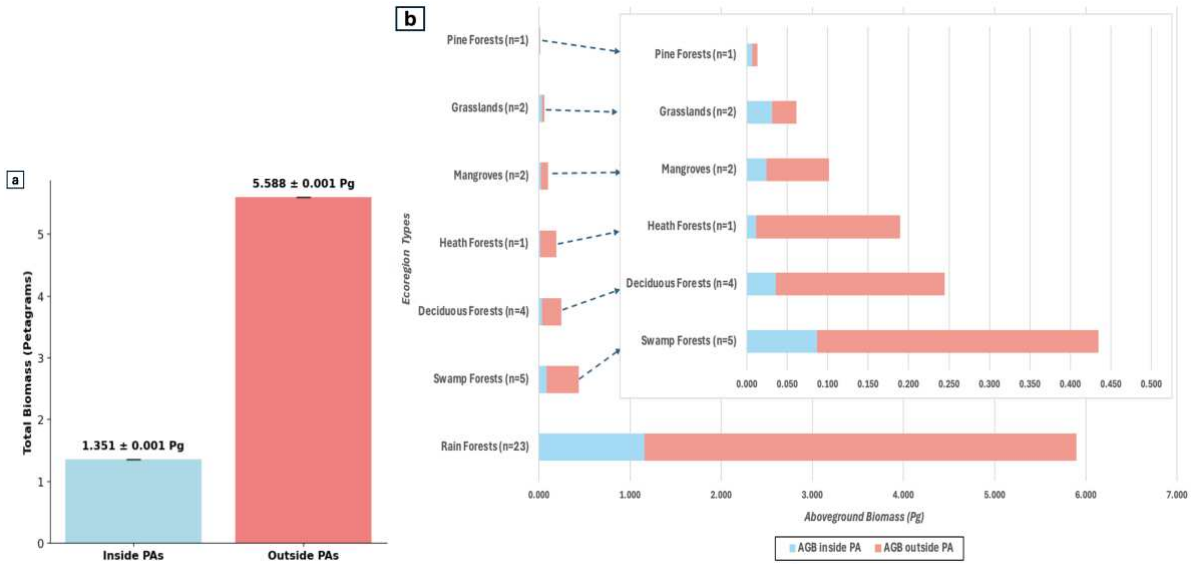


Figure 8: Protected area coverage and AGBD distribution of GEDI–TanDEM-X AGB hotspots across ecoregions..
(a) Proportion of AGB hotspots located inside versus outside protected areas, based on GEDI–TanDEM-X biomass predictions.
(b) Total aboveground biomass (Pg C) of AGB hotspots within and outside protected areas across different ecoregion types.

Our results show distributions of AGB within and outside PAs across different forest hotspot types (Figure 8b). This distribution can provide potential conservation insights about the 38 ecoregions in Indonesia. Rainforest ecoregions encompass the highest amount of the total biomass (5.9 Pg) where the majority (4.7 Pg) lies outside PAs, with only 1.2 Pg is inside PAs. This suggests significant vulnerability of high-biomass rainforest areas that currently lack formal protection. Swamp forests and deciduous forests also show a high proportion of AGB outside PAs, 0.4 Pg and 0.2 Pg respectively, compared to 0.1 Pg and 0.04 Pg inside PAs. Conversely, grasslands, pine forests, and mangroves have relatively higher proportional protection. Notably, grasslands and pine forests show a slightly higher AGB within PAs than outside, suggesting either higher protection status or designated PAs encompassing the concentration of biomass-rich areas in these ecoregions. The one heath forest in Indonesia, demonstrates the most alarming distribution, where more than 90% of the AGB is located outside PAs.

The structural diversity hotspots, identified using WSCI values, were also analyzed to determine their protection status within Indonesia's PAs. The ecosystem type based comparative assessment between the AGBD and structural diversity hotspots percentage within PAs (see Supplementary Figure S3), gives an insight of how the PAs in each forest type are currently protecting the derived hotspots for AGBD and Structural Diversity. Moreover, this ecoregion level comparison highlights which ecoregion contains more AGBD or structural diversity in the PAs.

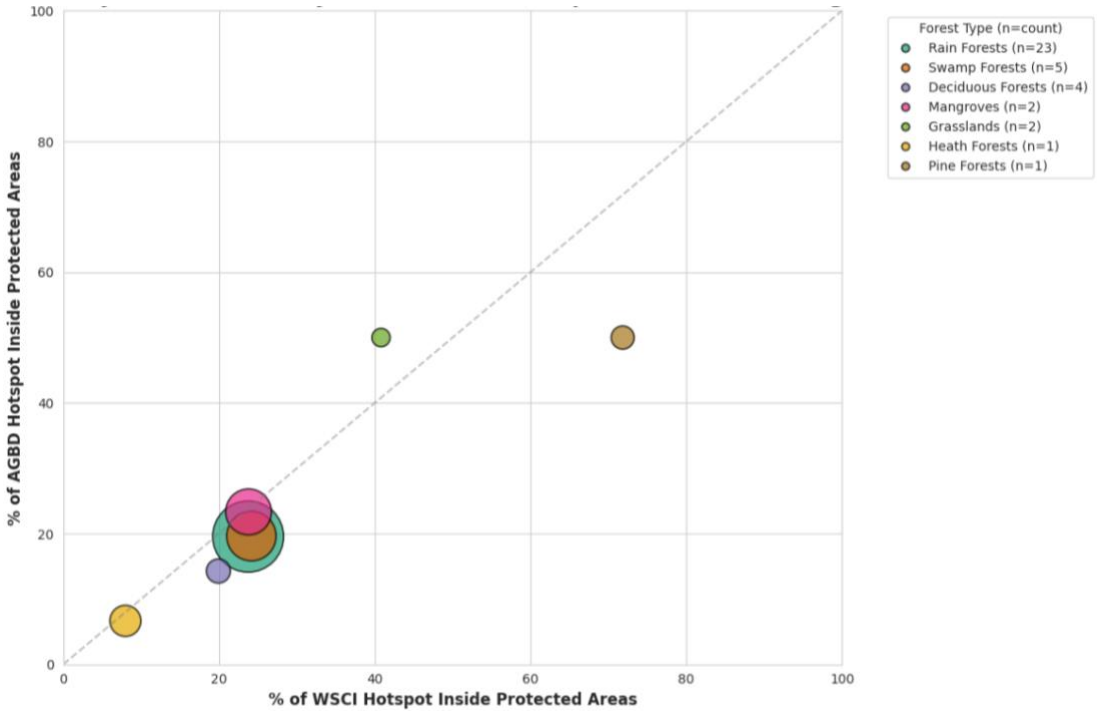


Figure 9: Comparison of protected area coverage of AGBD and WSCI hotspots across forest types in Indonesia.

The proportion of WSCI hotspots (x-axis) and AGBD hotspots located within protected areas across different forest types. Each point represents a forest type, with bubble size proportional to the total area and colours distinguishing forest ecosystem categories. The 1:1 line (dashed) indicates equal levels of protection coverage between structural diversity and biomass hotspots.

The distribution of WSCI and AGBD hotspots across forest types reveals substantial variation in PA coverage (Figure 9). Rainforests contain the largest extent of WSCI hotspots, yet only ~24% fall within PAs, while a similar proportion (~20%) of biomass hotspots are protected. Swamp forests and mangroves show comparable patterns, with ~24% of WSCI hotspots and ~20% of biomass hotspots located within PAs, respectively, highlighting consistently low protection across these wetland forest systems. Heath forests exhibit the lowest overall protection, with less

than 10% of both structural diversity and biomass hotspots falling inside PAs. In contrast, pine forests show relatively high protection, particularly for structural diversity (~72% WSCI hotspots inside PAs), while biomass protection remains lower (~50%). Grasslands also show higher relative protection compared to forested systems, with ~41% of WSCI hotspots and ~50% of biomass hotspots located within PAs. Deciduous forests display consistently low protection for both metrics (~20% WSCI and ~14% biomass).

3. Discussion

Our findings are consistent with previous studies which suggest the most critical conservation areas are not always contained by designated PAs and may require reassessment or expansion to better align with high-priority zones for biodiversity and carbon storage [53–55]. Similarly, in SEA and Indonesia, while PAs reduce carbon loss, large extents of rainforest AGB lie outside protection and under concession or land-use pressure [56,57]. As a result, failure to protect these high-AGB areas could lead to high amounts of carbon emissions if they are deforested, degraded or converted.

The ecoregions storing the most total AGB are Borneo lowland rainforests, Sumatran lowland rainforests and Sulawesi lowland rainforests. These ecoregion patterns are consistent with global AGB assessments and localized Indonesian studies that report similarly high mean AGB in intact rainforest ecoregions[5,53,58]. However, these high-biomass regions are not consistently aligned with PA coverage which indicates that key carbon-dense forest clusters extend beyond existing formal conservation boundaries. This spatial mismatch highlights the importance of hotspot-based prioritization rather than ecoregion-wide totals for identifying high-value carbon conservation areas.

Our spatial assessment of co-benefit areas reveals that AGBD and WSCI hotspots exhibit partial but asymmetric overlap, indicating that the two dimensions of forest condition are not spatially congruent. The spatial pattern of co-benefit areas shows a clear separation between carbon-rich forests and structurally complex forests across the landscape. This asymmetry indicates that structurally diverse forests are more frequently found outside high-carbon regions than the reverse. WSCI captures fine-scale three-dimensional canopy heterogeneity derived from GEDI waveform structure, including vertical layering, variation in crown height, and canopy gap dynamics [10,52]. Global GEDI-based analyses show that structural complexity is not restricted to high-biomass

forests, with relatively short or regenerating tropical forests also exhibiting elevated structural heterogeneity due to complex canopy organization [52]. Such conditions generate strong three-dimensional variability even in forests with comparatively lower biomass. Consequently, forest areas with the highest structural diversity do not always coincide spatially with the highest biomass stocks, a pattern consistent with our observed asymmetric hotspot overlap. The observed spatial mismatch between biomass and structural diversity hotspots further highlights the importance of evaluating how effectively existing PA networks capture co-benefit landscapes across Indonesia.

The largest share of unprotected co-benefit areas is >10 km from designated PA boundaries (Figure 4b). This spatial distribution is consistent with previous regional studies reporting that high-value forest areas are not always adequately captured within existing PA networks [53,54], suggesting limitations in the spatial representativeness of current PA design. This may influence their effectiveness in capturing high-value ecosystems. Barumun Wildlife Reserve (Figure 2b) protects a modest share of co-benefit areas within the Sumatran Montane and Lowland Rain Forests. Bogani Nani Wartabone National Park (Figure 2c) performs relatively well (see Supplementary Figure S7), aligning closely with co-benefit hotspots in the Sulawesi Montane and Lowland Rain Forests. In contrast, the cluster of PAs in the Lesser Sundas Deciduous Forests; Gunung Rinjani National Park (see Supplementary Figure S8), Kerandangan Nature Recreation Park, and Nuraksa Grand Forest Park (Figure 2d), contain no co-benefit areas despite overlapping with a structurally diverse ecoregion. Hence, re-evaluating the efficiency of existing PA coverage can result in positive conservation efforts made under Indonesia's FOLU Net Sink by 2030 by reducing potential forest reforestation and increasing sustainable forest management [59]. From a policy perspective, the identified co-benefit areas align strongly with Indonesia's FOLU Net Sink 2030 priorities, particularly in targeting high-carbon forests for protection and sustainable management, and integrating these spatial datasets into national planning could improve prioritization of conservation expansion and REDD+ interventions.

A substantial portion of co-benefit areas are relatively remote, although a notable fraction (~40%) lies within 10 km of roads (Figure 5). This suggests that a proportion of high-value forest areas are accessible and may face anthropogenic pressures, although vulnerability is also influenced by additional factors such as land concessions, agricultural expansion, and infrastructure development, which are key drivers of deforestation in Indonesia. The positive relationship between proximity to roads and elevated deforestation risk has been well established in previous research

where road expansion can increase access, selective logging, and subsequent clearing, thereby increasing carbon emissions risk [60,61]. In Indonesia, these pressures are often intensified by the expansion of oil palm plantations and forest logging, which have historically driven substantial forest loss, particularly in lowland rainforest regions [54,56]. This could potentially undermine the achievement of Indonesia's Nationally Determined Contributions (NDCs) targets under the Paris Agreement [62] if not effectively and sustainably managed.

A recent study also provides evidence that infrastructure development plans and ongoing road expansion in parts of Indonesia and Borneo will increase future pressure on currently remote high-AGB areas [63]. Human footprint analyses, which is closely related to the PA vulnerability, likewise shows rising pressure in PA buffer zones in Indonesia over recent decades where between 2012 and 2017 footprint increased from 0.4 to 77.3% around most of the national parks [64], consistent with our buffer-zone results. These studies support our interpretation that even relatively remote co-benefit hotspots could face growing risk if infrastructure and land-use pressures continue in Indonesia. In this context, aligning conservation planning with the 30×30 goal is critical, particularly given that a large proportion of high-carbon and structurally diverse forests in Indonesia remain outside existing protected area networks. While Indonesia has a substantial forest estate under protection and conservation designations, many high-value ecosystems remain unprotected or under other land-use categories. Currently, only ~12% of Indonesia's terrestrial land area is under formal protection, indicating a substantial proportion of land remains outside PA networks [65]. Our analysis on their buffer zones indicates that while the largest share remains >10 km from existing PA networks (Figure 4b), ~18% could be protected by strategic PA expansion. Strategic expansion, establishment of new PAs, or improved management of existing conservation areas targeting these co-benefit zones could significantly enhance both aboveground carbon storage and structural diversity (as a proxy of biodiversity), directly supporting Indonesia's climate mitigation and biodiversity conservation commitments.

While our co-benefit maps were designed to highlight conservation opportunities, these maps are not without error, and we acknowledge several limitations of the data and methods used in this study. First, the EO products used to map AGBD and WSCI have different temporal coverage. The biomass layer incorporates data from 2013–2018, whereas the structural diversity product used in this study was extracted only for 2020. This mismatch means that disturbances between 2013–2020 may not be fully reflected, and changes after 2020 are excluded. Second, this

study focuses on aboveground biomass and does not account for belowground carbon stocks, which is a key limitation in the Indonesian context where peatland ecosystems store substantial amounts of carbon belowground. Third, PA representation in this study is based on the WDPA dataset, which does not entirely encompass the diversity of conservation and land-use designations in Indonesia. Other forms of protection, including protected forests (hutan lindung), customary forests, and high conservation value (HCV) areas within production landscapes, may also contribute significantly to biodiversity conservation but are not explicitly included in this analysis. Finally, while global evaluations exist, there remains a lack of independent field or airborne validation in Southeast Asia, which increases the uncertainty in biomass products used in the study. Future annual products with consistent temporal coverage and regional validation can help address these issues.

4. Conclusion

We found that the majority of the high aboveground carbon and structurally diverse areas in Indonesia lie outside of current designated PAs. Rainforests exhibit the highest percentages of unprotected co-benefit areas that remain unprotected, followed closely by swamp forests and deciduous forests. These results raise important questions about the spatial effectiveness of existing protected area networks in capturing high-value ecosystems. These spatial priorities are directly relevant to Indonesia's FOLU Net Sink 2030 goals and can support more targeted implementation of REDD+ strategies by identifying high-carbon forests that are currently outside WDPA defined protected zones. Although this analysis focuses on Indonesia, the framework is transferable to other tropical forest regions where similar differences between carbon-rich ecosystems and PA coverage are expected.

While this work was based on the first satellite lidar designed to study Earth's forests, future satellite missions such as ESA BIOMASS and NASA-ISRO NISAR are expected to improve temporal monitoring of forest structure and biomass, enabling more dynamic assessments of carbon stocks and impact assessments of conservation and restoration activities. These missions will enable near real time structural monitoring of forest loss and degradation, thus strengthening monitoring capabilities of the hotspots identified in this work, and their potential future vulnerability to change. Our work presents a baseline by which future products and analyses can be compared, in the hope that expanded protected area networks will include higher percentages of

areas deemed high biomass and areas of high structural diversity that support biodiversity, and that these co-benefit areas are effectively preserved as long-term carbon stores and habitat refuges.

5. Methodology

5.1 Datasets and Study Area :

Remote Sensing Data

The GEDI instrument, launched by NASA on the International Space Station (ISS) in December 2018, is the first spaceborne lidar instrument which is optimized to measure ecosystem structure and provide high-quality measurements of forest vertical structure between 51.6° N & S latitude in temperate and tropical forests [10]. GEDI offers an unprecedented volume of 3D forest observations providing significantly more data than previous systems [66]. This instrument collects ~25 m footprint waveform data along orbital transects [10]. The recording of the vertical structure led to a calculation of AGBD for each footprint across all the transects which can be accessed through the GEDI Level 4A (L4A) product [67]. Structural diversity metrics, including WSCI, are obtained from the GEDI Level 4C (L4C) product and are used here to identify structural diversity hotspots [52]. Both products provide spatially explicit estimates along with associated uncertainty metrics [10,52].

However, due to the track distance between GEDI shots, the dataset does not provide continuous spatial coverage at high spatial resolution (<1km). Hence, producing products at finer resolution and wall-to-wall coverage requires fusion of GEDI lidar data with ancillary datasets. This fusion enables contiguous maps of forest biomass and structural diversity with higher accuracy and finer spatial resolution [68,69]. To address this limitation, this study uses two recently published GEDI-derived wall-to-wall datasets: one for forest biomass estimation and another for structural diversity mapping. For achieving the most effective fusion, the ancillary data with GEDI needs to be strongly correlated with forest structure. One of such data is spaceborne Interferometric Synthetic Aperture Radar (InSAR) which can be sensitive to forest vertical structure depending on wavelength, as radar backscatter interacts with different canopy components. Longer wavelengths (L- and P-band) are able to penetrate deeper into the canopy and are more strongly related to forest structure, whereas shorter wavelengths (e.g., X- and S-band) primarily respond to upper canopy layers, allowing derivation of canopy height and structure metrics [69]. In 2010, the German Aerospace Center (DLR) launched the first dual-platform (bistatic) InSAR mission – TerraSAR-X/TanDEM-X (TDX) [11]. Since the launch, TDX data has successfully been implemented to derive

forest structure (particularly height) over different terrains and environmental conditions [70–73]. Thus, it serves as a reliable secondary data for wall-to-wall product generation of high biomass and structural diversity co-benefit areas. Hence, a GEDI-TDX fusion product[74] is used in this research for accurately identifying all the high-AGBD areas of Indonesia (Table 1).

Complementing the biomass analysis, a wall-to-wall structural complexity product derived from GEDI L4C WSCI [52] and GEDI–SAR fusion (integrating Sentinel-1, ALOS PALSAR, and Copernicus DEM) is implemented to enable spatially continuous mapping of forest structural complexity beyond the native GEDI sampling footprint [68] (Table 1). The WSCI provides a single, interpretable metric of three-dimensional canopy structural complexity derived from GEDI observations, facilitating large-scale ecological assessments [52]. This dataset is used for mapping high priority structural diversity hotspots and co-benefit regions in each ecoregion level's top 10% threshold.

This study focuses on Indonesia, which is one of the largest holders of tropical forests globally and ranks among the top three countries in terms of tropical forest extent [75]. The country spans 38 ecoregions [76], within which we identify hotspots and co-benefit regions using both ecoregion-specific (Table 2) and national thresholds.The research used five datasets (summarised in Table 1) where GEDI derived wall-to-wall datasets act as primary dataset from where the co-benefit areas are obtained. It should be noted that the biomass dataset represents conditions from approximately 2013–2018, whereas we used the structural diversity dataset only for the year 2020. This temporal mismatch may introduce uncertainty in areas that experienced forest disturbance during this period.

Table 1: Data Information

Dataset Name	***Timeframe (used in this research)***	***Details***
GEDI-TDX Fusion Biomass Dataset [77]	2013-2018	100m resolution wall-to-wall raster
GEDI L4C Global Waveform Structural Complexity Index (WSCI) Fusion Product (Sentinel-1, PALSAR-2 and CopernicusDEM) [78]	2020	25m resolution wall-to-wall raster
World Ecoregions by WWF [76,79]	2001	Boundary files extracted from World Wildlife Fund(WWF) Terrestrial Biomes

World Database on Protected Areas (WDPA) [80]	01/2024 version	United Nations Environmental Program (UNEP) International Union for Conservation of Nature (IUCN)
OpenStreetMap(OSM) Major Roads of Indonesia [81]	2024	Road data extracted from Humanitarian Data Exchange(HDX) of HOTOSM(Humanitarian OpenStreetMap Team)

5.2 Data Processing and Analysis:

The data processing of this study was conducted with an estimated classification system defined to detect ecoregion-based thresholds of highest AGBD and WSCI (Table 2). Specifically, for each ecoregion, all quality-filtered AGBD and WSCI estimates were extracted from the wall-to-wall datasets (Table 1). Key hotspot areas were then defined using a percentile-based approach, where grid cells exceeding the 90th percentile (top 10%) of the respective ecoregion's value distribution were classified as hotspots (Table 2). The percentile-based threshold approach allows hotspot identification relative to local ecological conditions. The 90th percentile threshold was selected to capture the highest-value areas while maintaining sufficient spatial coverage for analysis. Biomass(AGBD)-based hotspots were identified at 100 m resolution using AGBD values, while structural diversity–based hotspots were identified at 25 m resolution using WSCI values. This ecoregion-specific thresholding ensures that hotspot identification is relative to local ecological conditions and allows the methodology to be directly replicated for any region with comparable input data. As each ecoregion has their own distinct threshold (i.e., rain forests containing higher values of AGBD vs grasslands and mangroves, which contains less), the goal here is to prioritize their unique nature and have co-benefit areas per ecoregion that can be high priority conservation areas. To provide a broader context, a national-level hotspot and co-benefit analysis was also done using the top 10% of AGBD and WSCI values across Indonesia. The results presented in the main manuscript are based on ecoregion-specific thresholds, while the national threshold-based results are provided in the Supplementary Information.

Finally, the co-benefit areas were derived with an overlap analysis using previously obtained and resampled AGBD and WSCI hotspots (Figure 1). All the data processing was done on NASA Multi-Mission Algorithm and Analysis Platform (MAAP).

Table 2: Classification Definitions

Classification Type	*Description*
1. Ecoregion Specific biomass Threshold based key hotspot areas	100m cells where hotspots cells meet the top 10% AGBD threshold of the respective ecoregion's all quality estimates
2. Structural Diversity based key hotspot areas	25m cells where hotspots cells meet the top 10% WSCI threshold of the respective ecoregion's all quality estimates
3. National Hotspots of biomass and structural diversity	100m (AGBD) and 25m (WSCI) cells where hotspots cells meet the top 10% threshold of the entire country's dataset

5.3 AGBD and Structural Diversity based hotspots identification:

GEDI-TDX based AGBD Hotspots Identification:

For the identification of AGBD hotspots in Indonesia, a GEDI–TanDEM-X (GEDI-TDX) fusion raster product was utilized which integrates GEDI L4A aboveground biomass estimates with structural metrics derived from TanDEM-X interferometric synthetic aperture radar (SAR) data (Figure 1). The fusion product represents the temporal range of 2013-2018, providing wall-to-wall coverage at a spatial resolution of 100 meters.

To facilitate ecosystem-specific assessments, the entire country's dataset was divided into 38 ecoregions based on the boundary dataset derived from WWF Terrestrial Ecoregions of the World [79]. Within each ecoregion, we identified AGBD "hotspot" cells as those with AGBD values greater than or equal to the 90th percentile of that ecoregion's biomass distribution through steps denoted in Figure 1. This relative thresholding approach ensures that hotspot definitions are ecologically adaptive, so that not all hotspot areas are found within the highest biomass ecoregion (typically tropical rainforest) and thus the resulting products can inform conservation across each ecosystem type.

A similar method was followed for national level AGBD hotspots identification where top 10% cells were selected based on the entire country's threshold.

GEDI-L4C Fusion Structural Complexity hotspots Identification:

The same methods, as mentioned in AGBD hotspots identification, were applied to WSCI, classifying pixels as hotspots that are in the top 10% threshold per ecoregion (Figure 1). The 90th

percentile of WSCI values was computed from non-zero, valid pixels. Structural diversity hotspots were then defined as all 25 m cells with WSCI values greater than or equal to this threshold.

5.4 Assessment of the AGB proportion of protected vs. unprotected areas in each ecoregion and whole country

After identifying high-priority co-benefit zones based on biomass and structural diversity, these cells were compared against the PAs. In this study, PAs refer to conservation forest categories represented in the World Database on Protected Areas (WDPA) [80], which form the country's primary legal framework for biodiversity protection.

The proportion of hotspot cells located within and outside PAs was quantified, and the percentage distribution for each ecoregion was derived. Additionally, the total aboveground biomass (AGB) within protected and non-protected areas was calculated using the following formula:

Total AGB = Mean AGB Cell Area*

Since each cell represents 1ha with the mean AGB value, the values of all the hotspots cells were added, yielding the final AGB estimates. Uncertainty estimates from the biomass product were also incorporated, with pixel-level uncertainties aggregated to derive uncertainty for the total AGB estimates.

5.5 Identification and PA Assessment of Co-Benefit Areas in Indonesia:

For the identification of areas that are high in both aboveground carbon and structural diversity, termed as "co-benefit" areas, the AGBD and WSCI hotspot rasters were overlaid. As the WSCI hotspots file were 25m in resolution, they were resampled to 100m cells using average mean of nearby cells. This aggregation represents the mean fine-scale (25 m) structural complexity within each 100m cell, rather than structural complexity explicitly defined at the 1 ha scale. Given that WSCI was developed for fine-resolution characterization, its scaling behavior across spatial resolutions is not assumed to be linear.

After the overlay, 100m co-benefit cells were derived which exceeded the 90th percentile threshold in both layers within each ecoregion. National level hotspots were also resampled and overlaid similarly to detect country level co-benefit areas.

The distribution of identified co-benefit area cells relative to PAs were then assessed with the WDPA layer. The preliminary risk analysis was performed using the cells' distance to nearby major roads, which were derived from OpenStreetMap datasets [81].

6. Data availability

The data generated in this study, including processed spatial layers of aboveground biomass density (AGBD) hotspots, waveform structural complexity index (WSCI) hotspots, co-benefit areas, protected-area overlap analyses, road-proximity analyses, ecoregion-level summary statistics, and the source data underlying all main and supplementary figures, will be deposited in a publicly accessible repository upon acceptance of the manuscript. During peer review, these derived datasets are available from the corresponding author upon request.

This study used the following publicly available and third-party datasets:

The GEDI L4C Global Waveform Structural Complexity Index (WSCI) fusion product (25 m spatial resolution; 2020) is publicly available through the NASA Land Processes Distributed Active Archive Center (LP DAAC): (https://www.earthdata.nasa.gov/data/catalog/ornl-cloud-gedi-l4c-wsci-fusion-2474-2)

Terrestrial ecoregion boundaries were obtained from the World Wildlife Fund(WWF) Terrestrial Ecoregions of the World dataset (https://databasin.org/datasets/68635d7c77f1475f9b6c1d1dbe0a4c4c/).

Protected-area boundaries were obtained from the January 2024 release of the World Database on Protected Areas(WDPA), managed by the UN Environment Programme(UNEP) World Conservation Monitoring Centre and the International Union for Conservation of Nature(IUCN) (www.protectedplanet.net).

Major road network data for Indonesia were obtained from OpenStreetMap(OSM) via the Humanitarian Data Exchange and the Humanitarian OpenStreetMap Team (https://data.humdata.org/organization/hot).

The GEDI–TanDEM-X fusion biomass product for Indonesia (100 m spatial resolution; 2013–2018), developed under NASA's Carbon Monitoring System(CMS) Phase II, was used under a data-sharing agreement with the data providers and is not yet publicly available. Public release through a NASA Distributed Active Archive Center is anticipated. In the interim, access to this dataset may be requested from the data providers, subject to their approval and applicable data-use conditions. Details of the dataset and its methodological framework are provided in the original publication.

All source data underlying the figures and statistical analyses will be provided with the published article.

Code availability

Custom code used for data processing, geospatial analyses, statistical analyses, and figure generation is publicly available at NASA Earthdata Github Repository: https://repo.maap-project.org/pbasak/gedi-indonesia-cobenefits/.
A permanent archived release with a DOI will be created upon acceptance of the manuscript.

7. Acknowledgements

This work was supported by NASA through the Future Investigators in NASA Earth and Space Science and Technology (FINESST) program (Award No. 80NSSC24K1597) and GEDI science team grant 80NSSC24K0. This support enabled the research design, analysis, and interpretation presented in this study.

The datasets used in this study were developed with support from NASA's Carbon Monitoring System (CMS) grant 80NSSC23K1256. In particular, we acknowledge the Global Ecosystem Dynamics Investigation (GEDI) mission science team for providing access to these high-quality datasets that made this work possible. We also acknowledge the funding from NASA contract NNL 15AA03C for the development and execution of the GEDI mission.

The authors also gratefully acknowledge the NASA-ESA Multi-mission Algorithm and Analysis Platform (MAAP) which enabled all data access, compute, and support from NASA MAAP data and platform teams.

References:

1. IPCC. *Global Warming of 1.5 ºC —*. https://www.ipcc.ch/sr15/ (2018).
2. Pecl, G. T. *et al.* Biodiversity redistribution under climate change: Impacts on ecosystems and human well-being. *Science* **355**, eaai9214 (2017).
3. UNEP, U. N. E. P. & FAO, F. and A. O. of the U. The State of the World's Forests 2020: Forests, Biodiversity and People. https://wedocs.unep.org/handle/20.500.11822/32472 (2020).
4. Mo, L. *et al.* Integrated global assessment of the natural forest carbon potential. *Nature* **624**, 92–101 (2023).
5. Pan, Y., Birdsey, R. A., Phillips, O. L. & Jackson, R. B. The Structure, Distribution, and Biomass of the World's Forests. *Annu. Rev. Ecol. Evol. Syst.* **44**, 593–622 (2013).
6. Santoro, M. *et al.* The global forest above-ground biomass pool for 2010 estimated from high-resolution satellite observations. *Earth Syst. Sci. Data* **13**, 3927–3950 (2021).
7. Mulatu, K. A., Mora, B., Kooistra, L. & Herold, M. Biodiversity Monitoring in Changing Tropical Forests: A Review of Approaches and New Opportunities. *Remote Sens.* **9**, 1059 (2017).
8. Brodie, J. F. *et al.* Defaunation impacts on the carbon balance of tropical forests. *Conserv. Biol.* **39**, e14414 (2025).
9. Damon Matthews, H. *et al.* An integrated approach to quantifying uncertainties in the remaining carbon budget. *Commun. Earth Environ.* **2**, 7 (2021).
10. Dubayah, R. *et al.* The Global Ecosystem Dynamics Investigation: High-resolution laser ranging of the Earth's forests and topography. *Sci. Remote Sens.* **1**, 100002 (2020).
11. Zink, M., Krieger, G., Fiedler, H. & Moreira, A. The TanDEM-X mission: Overview and status. in *2007 IEEE International Geoscience and Remote Sensing Symposium* 3944–3947 (2007). doi:10.1109/IGARSS.2007.4423711.
12. Ramachandran, N., Saatchi, S., Tebaldini, S., d'Alessandro, M. M. & Dikshit, O. Mapping tropical forest aboveground biomass using airborne SAR tomography. *Sci. Rep.* **13**, 6233 (2023).
13. Brassard, B. W., Chen, H. Y. H., Wang, J. R. & Duinker, P. N. Effects of time since stand-replacing fire and overstory composition on live-tree structural diversity in the boreal forest of central Canada. *Can. J. For. Res.* **38**, 52–62 (2008).

14. Ishii, H. T., Tanabe, S. & Hiura, T. Exploring the Relationships Among Canopy Structure, Stand Productivity, and Biodiversity of Temperate Forest Ecosystems. *For. Sci.* **50**, 342–355 (2004).
15. MacArthur, R. H. & Wilson, E. O. *The Theory of Island Biogeography*. (Princeton University Press, 2001).
16. Müller, J. *et al.* LiDAR-derived canopy structure supports the more-individuals hypothesis for arthropod diversity in temperate forests. *Oikos* **127**, 814–824 (2018).
17. Simpson, E. H. Measurement of Diversity. *Nature* **163**, 688–688 (1949).
18. Storch, F. *et al.* Linking structure and species richness to support forest biodiversity monitoring at large scales. *Ann. For. Sci.* **80**, 3 (2023).
19. Cadieux, P. *et al.* Old forest structural development drives complexity of nest webs in a naturally disturbed boreal mixedwood forest landscape. *Front. For. Glob. Change* **6**, (2023).
20. Bergman, K.-O. *et al.* From clear-cuts to nature reserves: saproxylic beetle diversity and deadwood availability in Norway spruce (Picea abies L.) stands in southern Sweden. *Ann. For. Sci.* **82**, 37 (2025).
21. Ali, A. Forest stand structure and functioning: Current knowledge and future challenges. *Ecol. Indic.* **98**, 665–677 (2019).
22. Concha, V. C., Caviedes, J., Novoa, F. J., Altamirano, T. A. & Ibarra, J. T. Structural complexity is a better predictor than single habitat attributes of understory bird densities in Andean temperate forests. *Ornithol. Appl.* **125**, duad035 (2023).
23. Xu, J. *et al.* Avian diversity across guilds in North America versus vegetation structure as measured by the Global Ecosystem Dynamics Investigation (GEDI). *Remote Sens. Environ.* **315**, 114446 (2024).
24. Heidrich, L. *et al.* Heterogeneity–diversity relationships differ between and within trophic levels in temperate forests. *Nat. Ecol. Evol.* **4**, 1204–1212 (2020).
25. Bennett, L. T. *et al.* Assessing fire impacts on the carbon stability of fire-tolerant forests. *Ecol. Appl.* **27**, 2497–2513 (2017).
26. CBD, (Convention on Biological Diversity). *Report of the Conference of the Parties to the Convention on Biological Diversity on the Second Part of Its Fifteenth Meeting*. https://www.cbd.int/doc/c/f98d/390c/d25842dd39bd8dc3d7d2ae14/cop-15-17-en.pdf (2022).

27. Chen, C. *et al.* Global camera trap synthesis highlights the importance of protected areas in maintaining mammal diversity. *Conserv. Lett.* **15**, e12865 (2022).
28. Geldmann, J., Manica, A., Burgess, N. D., Coad, L. & Balmford, A. A global-level assessment of the effectiveness of protected areas at resisting anthropogenic pressures. *Proc. Natl. Acad. Sci.* **116**, 23209–23215 (2019).
29. Watson, J. E. M., Dudley, N., Segan, D. B. & Hockings, M. The performance and potential of protected areas. *Nature* **515**, 67–73 (2014).
30. Dinerstein, E. *et al.* A Global Deal For Nature: Guiding principles, milestones, and targets. *Sci. Adv.* **5**, eaaw2869 (2019).
31. Jung, M. *et al.* Areas of global importance for conserving terrestrial biodiversity, carbon and water. *Nat. Ecol. Evol.* **5**, 1499–1509 (2021).
32. Soto-Navarro, C. *et al.* Mapping co-benefits for carbon storage and biodiversity to inform conservation policy and action. *Philos. Trans. R. Soc. B Biol. Sci.* **375**, 20190128 (2020).
33. Shi, H. *et al.* Global protected areas boost the carbon sequestration capacity: Evidences from econometric causal analysis. *Sci. Total Environ.* **715**, 137001 (2020).
34. Wolf, C., Levi, T., Ripple, W. J., Zárrate-Charry, D. A. & Betts, M. G. A forest loss report card for the world's protected areas. *Nat. Ecol. Evol.* **5**, 520–529 (2021).
35. Yang, H. *et al.* A global assessment of the impact of individual protected areas on preventing forest loss. *Sci. Total Environ.* **777**, 145995 (2021).
36. Chen, J. *et al.* Microclimate in Forest Ecosystem and Landscape Ecology: Variations in local climate can be used to monitor and compare the effects of different management regimes. https://dx.doi.org/10.2307/1313612 (1999).
37. Fuente, B. de la *et al.* Land productivity dynamics in and around protected areas globally from 1999 to 2013. *PLOS ONE* **15**, e0224958 (2020).
38. Huang, Y. *et al.* Impacts of species richness on productivity in a large-scale subtropical forest experiment. *Science* **362**, 80–83 (2018).
39. Goldstein, A. *et al.* Protecting irrecoverable carbon in Earth's ecosystems. *Nat. Clim. Change* **10**, 287–295 (2020).
40. Harris, N. L. *et al.* Global maps of twenty-first century forest carbon fluxes. *Nat. Clim. Change* **11**, 234–240 (2021).

41. Araza, A. *et al.* A comprehensive framework for assessing the accuracy and uncertainty of global above-ground biomass maps. *Remote Sens. Environ.* **272**, 112917 (2022).
42. Duncanson, L. *et al.* The Importance of Consistent Global Forest Aboveground Biomass Product Validation. *Surv. Geophys.* **40**, 979–999 (2019).
43. Duncanson, L. *et al.* The effectiveness of global protected areas for climate change mitigation. *Nat. Commun.* **14**, 2908 (2023).
44. Government of Indonesia. *Law No. 41/1999 on Forestry*. https://www.flevin.com/id/lgso/translations/Laws/Law%20No.%2041%20of%201999%20on%20Forestry.pdf (1999).
45. Sodhi, N. S. *et al.* The state and conservation of Southeast Asian biodiversity. *Biodivers. Conserv.* **19**, 317–328 (2010).
46. Stibig, H.-J., Achard, F., Carboni, S., Raši, R. & Miettinen, J. Change in tropical forest cover of Southeast Asia from 1990 to 2010. *Biogeosciences* **11**, 247–258 (2014).
47. Santoro, A., Piras, F. & Yu, Q. Spatial analysis of deforestation in Indonesia in the period 1950–2017 and the role of protected areas. *Biodivers. Conserv.* https://doi.org/10.1007/s10531-023-02679-8 (2023) doi:10.1007/s10531-023-02679-8.
48. Brun, C. *et al.* Analysis of deforestation and protected area effectiveness in Indonesia: A comparison of Bayesian spatial models. *Glob. Environ. Change* **31**, 285–295 (2015).
49. Curran, L. M. *et al.* Lowland Forest Loss in Protected Areas of Indonesian Borneo. *Science* **303**, 1000–1003 (2004).
50. Fuller, D. O., Jessup, T. C. & Salim, A. Loss of Forest Cover in Kalimantan, Indonesia, Since the 1997–1998 El Niño. *Conserv. Biol.* **18**, 249–254 (2004).
51. Poor, E. E., Frimpong, E., Imron, M. A. & Kelly, M. J. Protected area effectiveness in a sea of palm oil: A Sumatran case study. *Biol. Conserv.* **234**, 123–130 (2019).
52. de Conto, T., Armston, J. & Dubayah, R. Characterizing the structural complexity of the Earth's forests with spaceborne lidar. *Nat. Commun.* **15**, 8116 (2024).
53. Gaveau, D. L. A. *et al.* Reconciling Forest Conservation and Logging in Indonesian Borneo. *PLOS ONE* **8**, e69887 (2013).
54. Margono, B. A., Potapov, P. V., Turubanova, S., Stolle, F. & Hansen, M. C. Primary forest cover loss in Indonesia over 2000–2012. *Nat. Clim. Change* **4**, 730–735 (2014).

55. Venter, O. *et al.* Bias in protected-area location and its effects on long-term aspirations of biodiversity conventions. *Conserv. Biol. J. Soc. Conserv. Biol.* **32**, 127–134 (2018).
56. Abood, S. A., Lee, J. S. H., Burivalova, Z., Garcia-Ulloa, J. & Koh, L. P. Relative Contributions of the Logging, Fiber, Oil Palm, and Mining Industries to Forest Loss in Indonesia. *Conserv. Lett.* **8**, 58–67 (2015).
57. Graham, V. *et al.* Southeast Asian protected areas are effective in conserving forest cover and forest carbon stocks compared to unprotected areas. *Sci. Rep.* **11**, 23760 (2021).
58. Baccini, A. *et al.* Tropical forests are a net carbon source based on aboveground measurements of gain and loss. *Science* **358**, 230–234 (2017).
59. Ministry of Environment and Forestry. *Operational Plan Indonesia's FOLU Net Sink 2030*. 168 https://planologi.kehutanan.go.id/assets/img/publication/BUKU_RENOPS_FOLU_NETSINK_2030_(English).pdf (2022).
60. Barber, C. P., Cochrane, M. A., Souza, C. M. & Laurance, W. F. Roads, deforestation, and the mitigating effect of protected areas in the Amazon. *Biol. Conserv.* **177**, 203–209 (2014).
61. Laurance, W. F., Goosem, M. & Laurance, S. G. W. Impacts of roads and linear clearings on tropical forests. *Trends Ecol. Evol.* **24**, 659–669 (2009).
62. Republic of Indonesia. *UNFCC Enhanced Nationally Determined Contribution(NDC): Republic of Indonesia*. https://unfccc.int/sites/default/files/NDC/2022-09/23.09.2022_Enhanced%20NDC%20Indonesia.pdf (2022).
63. Alamgir, M. *et al.* Infrastructure expansion challenges sustainable development in Papua New Guinea. *PLOS ONE* **14**, e0219408 (2019).
64. Dwiyahreni, A. A. *et al.* Changes in the human footprint in and around Indonesia's terrestrial national parks between 2012 and 2017. *Sci. Rep.* **11**, 4510 (2021).
65. World Bank. World Development Indicators: Terrestrial protected areas (% of land area). (2024).
66. Joshi, N. *et al.* Understanding 'saturation' of radar signals over forests. *Sci. Rep.* **7**, 3505 (2017).
67. Dubayah, R. *et al.* GEDI launches a new era of biomass inference from space. *Environ. Res. Lett.* **17**, 095001 (2022).

68. de Conto, T., Armston, J. & Dubayah, R. Scalable deep fusion of spaceborne lidar and synthetic aperture radar for global forest structural complexity mapping. *Mach. Learn. Earth* **2**, 015002 (2025).
69. Qi, W. *et al.* Improved forest height estimation by fusion of simulated GEDI Lidar data and TanDEM-X InSAR data. *Remote Sens. Environ.* **221**, 621–634 (2019).
70. Kugler, F., Schulze, D., Hajnsek, I., Pretzsch, H. & Papathanassiou, K. P. TanDEM-X Pol-InSAR Performance for Forest Height Estimation. *IEEE Trans. Geosci. Remote Sens.* **52**, 6404–6422 (2014).
71. Lee, S.-K. & Fatoyinbo, T. E. TanDEM-X Pol-InSAR Inversion for Mangrove Canopy Height Estimation. *IEEE J. Sel. Top. Appl. Earth Obs. Remote Sens.* **8**, 3608–3618 (2015).
72. Sadeghi, Y., St-Onge, B., Leblon, B. & Simard, M. Canopy Height Model (CHM) Derived From a TanDEM-X InSAR DSM and an Airborne Lidar DTM in Boreal Forest. *IEEE J. Sel. Top. Appl. Earth Obs. Remote Sens.* **9**, 381–397 (2016).
73. Treuhaft, R. *et al.* Tropical-Forest Biomass Estimation at X-Band From the Spaceborne TanDEM-X Interferometer. *IEEE Geosci. Remote Sens. Lett.* **12**, 239–243 (2015).
74. Qi, W. *et al.* Mapping large-scale pantropical forest canopy height by integrating GEDI lidar and TanDEM-X InSAR data. *Remote Sens. Environ.* **318**, 114534 (2025).
75. FAO, F. and A. O. of the U. *Global Forest Resources Assessment 2020: Main Report*. https://openknowledge.fao.org/items/d6f0df61-cb5d-4030-8814-0e466176d9a1 (2020).
76. World Wildlife Fund (WWF). WWF Terrestrial Ecoregions of the World (TEOW). (2004).
77. Dubayah, R. *et al.* Pantropical Forest Height and Biomass from GEDI and TanDEM-X Data Fusion. ORNL Distributed Active Archive Center https://doi.org/10.3334/ORNLDAAC/2298 (2023).
78. de Conto, T., Armston, J. & Dubayah, R. GEDI L4C Global Waveform Structural Complexity Index (WSCI) Fusion Product, Version 2. ORNL Distributed Active Archive Center. https://doi.org/10.3334/ORNLDAAC/2474 (2026).
79. Olson, D. M. *et al.* Terrestrial Ecoregions of the World: A New Map of Life on Earth: A new global map of terrestrial ecoregions provides an innovative tool for conserving biodiversity. *Biogeoscience* **51**, 933–938 (2001).
80. UNEP-WCMC & IUCN. *Protected Planet: The World Database on Protected Areas (WDPA)*. (2026).

81. OSM. Humanitarian OpenStreetMap Team (HOT) Humanitarian Data | 2024 Datasets | HDX. https://data.humdata.org/organization/hot (2024).

Supplementary Files

This is a list of supplementary files associated with this preprint. Click to download.

- SupplementaryMaterials.pdf